

Application Note

IoT debug gets a boost from true differential probing

This time we consider how a new differential input oscilloscope, the PicoScope 4444, helps debug a typical DC/DC converter designed to provide power in Internet of Things (IoT) applications.

A recent article [<https://www.picotech.com/library/application-note/how-true-differential-scope-inputs-boost-probing-safety-and-precision>] explained the benefits of differential probing, namely that of allowing engineers to safely probe important system signals unavailable to conventional, single-ended scopes and probes.

This benefit arises by eliminating the ground return path, which not only crushes floating signals but can also lead to systems sourcing enough current to destroy parts of the circuit, as well as potentially harming anyone unlucky enough to be caught out! As we will show, beyond the safety benefits, differential probing can give engineers insights into contemporary low-voltage circuits.

Introducing a versatile IoT battery regulator

The simple battery regulator circuit from Intersil (fig. 1) illustrates this and makes an interesting test case for this article.

At first glance, it is not apparent if the inductor L_1 is grounded or floating (fig. 1b). Inductor current is determined by switch settings, which in turn are determined by absolute levels of V_{IN} , V_{OUT} and output loading.

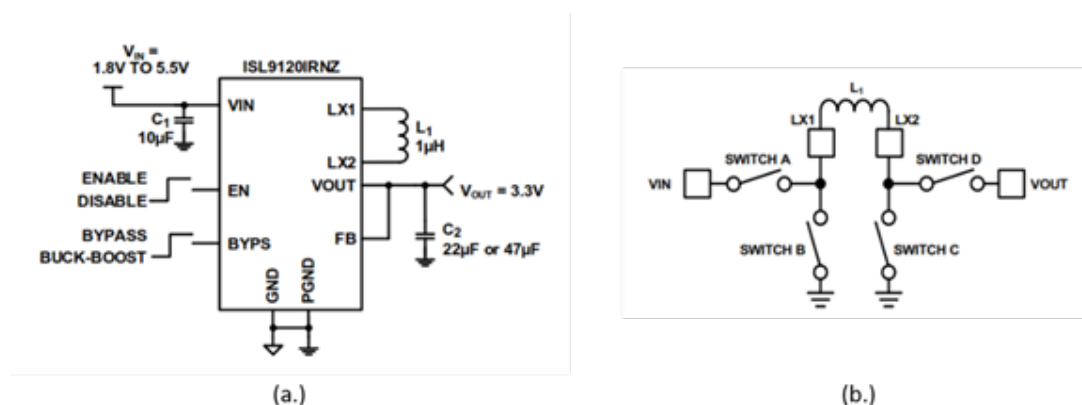


Figure 1 PFM mode battery regulator IC

ISL9120 Introduction

The ISL9120 is a hysteretic, multi-mode battery voltage switching regulator which operates in buck, boost or pass-through modes. As input voltage falls, the device swaps modes to maintain regulation, squeezing maximum operating life out of a given battery. The operating range suits many modern battery chemistries with a range between 1.8 and 5.5 V. The device can drive up to 800 mA into a load and requires a minimal number of external components, of which a small power inductor and output capacitor are key.

Switching basics

A switcher's primary benefit is energy-efficient conversion. The part under the lens here claims headline efficiency of 98% and an ability to maintain it above 85% under all conditions (see fig. 2). Achieving this feat is down to the hysteretic PFM (pulse frequency modulation) switching approach, which helps sustain efficiency even at light loads.

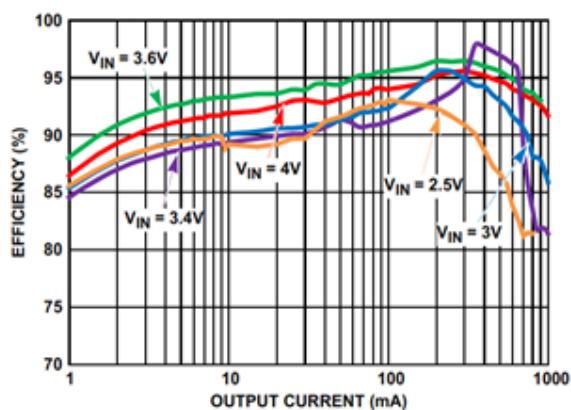


Figure 1 Conversion efficiency of ISL9120 (Courtesy Intersil)

Switching regulators use power inductors as their main energy storage element. Operation relies on transferring 'buckets' of energy from the input to the output side of the circuit. The amount of energy transferred each switch cycle is a function of the switching rate and the inductor size. In the circuit under inspection, a tiny surface-mount inductor does the job.

About the test setup

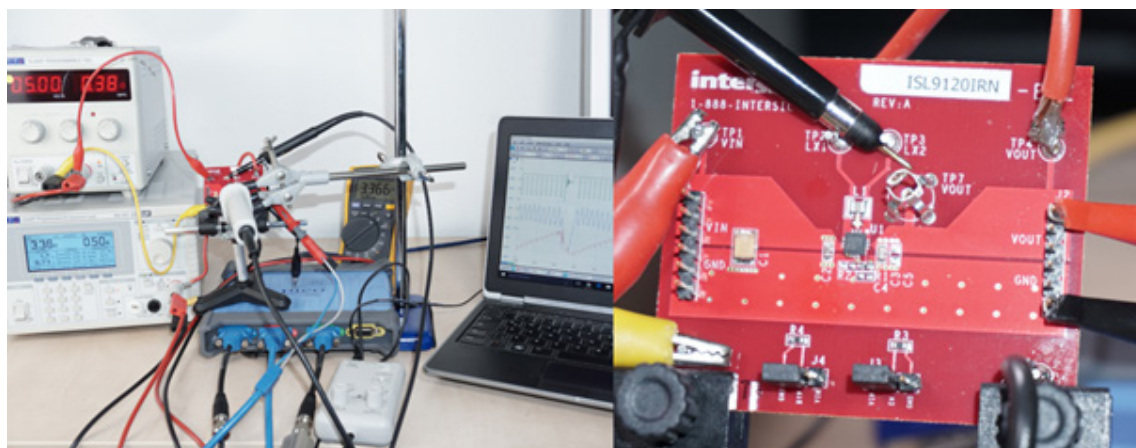


Figure 2 Test setup and close-up of ISL9120 evaluation board showing inductor probing points (TP2 & TP3)

The twin images above show the test set-up on the left and the Intersil evaluation board to the right. Note that the scope probe placed across the inductor at TP2 & TP3 (upper middle portion of the PCB) exploits the 'pin and barrel' probing method to minimize lead length difference between the probe poles – an important step in reducing ringing.

Supplier	Model No:	Description
AimTTi	EL302P	Programmable 0 to 30 V 2 A PSU
AimTTi	LD400P	Programmable 400 W electronic load (up to 30 A)
AimTTi	Iprober 520	Positional current probe (5 MHz, 20 A)
Fluke	177	True RMS DVM
Intersil	ISL9120IRN-EVZ	ISL9120 Evaluation board
Pico Technology	PicoScope 4444	20 MHz quad differential input, USB scope with 441 diff probes & TA271 (BNC to D-sub) adapters.

Table 1 Test gear list

This setup comprises standard lab equipment listed in Table 1, though perhaps the current sensing talents of the I-prober may not be available to everyone. This current probe features a novel magnetic sensor which allows direct current measurement, without the need to break the circuit and introduce a sense resistor. This is very helpful, as the Intersil board did not include a bridge for a low-ohmic sense resistor, thus making current measurement trickier than it needed to be.

Let's start probing

Four internal IC power switches surround the inductor, determining current flow (fig. 1-b). Considering all the switch combinations, it's difficult to unpick what instantaneous voltages might exist across it. The first trace below (fig. 4) overlays three important circuit signals, demonstrating the complex switching waveforms typical of such a circuit:

- **Red:** output voltage ripple (AC coupled)
- **Green:** inductor differential voltage (DC coupled)
- **Blue:** inductor current waveform (AC coupled)

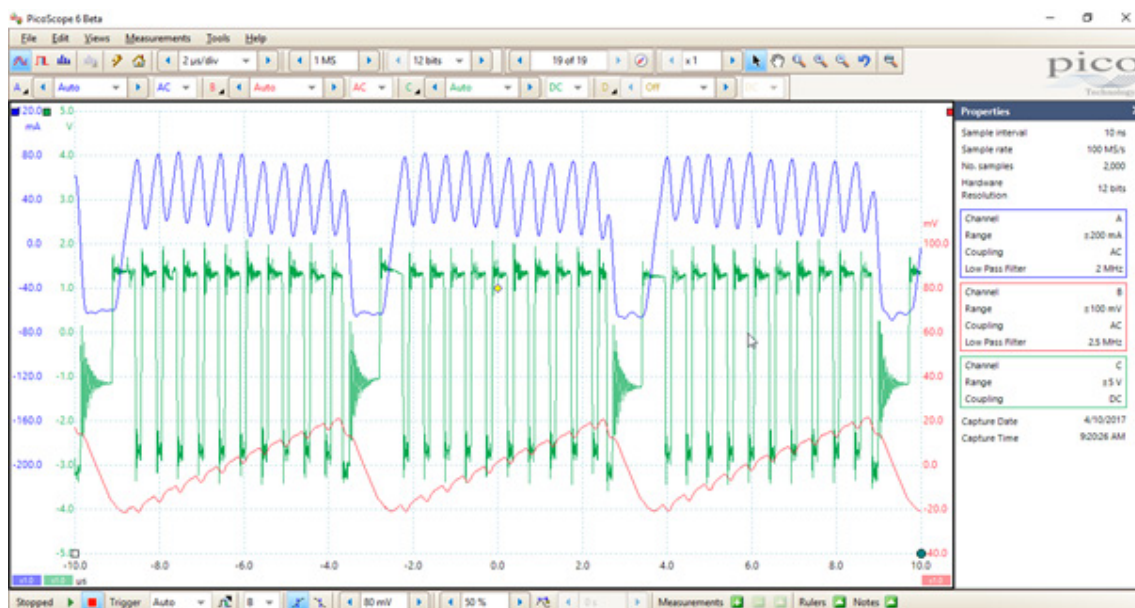


Figure 3 Initial waveforms captured on ISL9120 evaluation board overlaid

From here on, we focus solely on what is happening within the inductor (pins LX1 and LX2) and how that affects output voltage.

All three operating modes are now considered:

- Inductor voltage & current and output ripple under step-down conditions
- Inductor voltage & current and output ripple under step-up conditions
- Inductor voltage & current and output ripple in bypass mode

Step-down operation ($V_{IN} > V_{OUT}$)

The following trace was measured under the following static conditions:

- Set-up: $V_{in} = 5\text{ V}$, $V_{OUT} = 3.4\text{ V}$ and $I_{OUT} = 500\text{ mA}$
- Traces:
 - o **Red:** output voltage ripple (AC coupled)
 - o **Green:** inductor differential voltage (DC coupled)
 - o **Blue:** inductor current

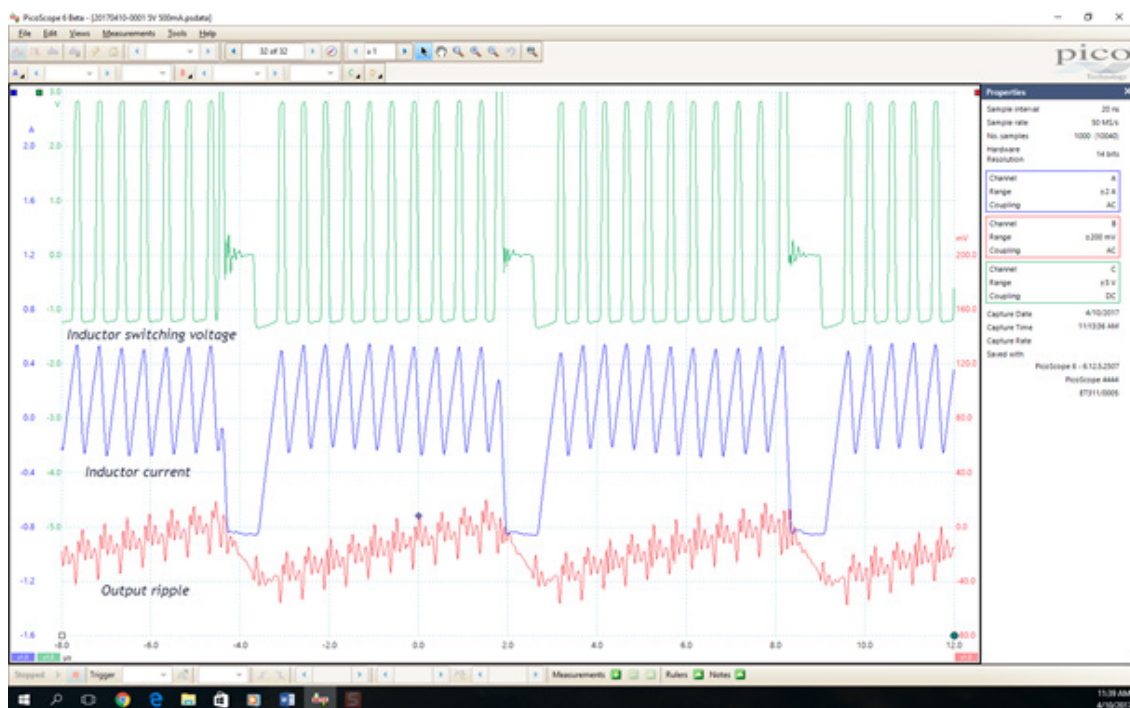


Figure 4 Step-down operation ($V_{in} = 5\text{ V}$, $V_{out} = 3.4\text{ V}$ and $I_{out} = 500\text{ mA}$)

The waveforms clarify circuit operation. The green trace shows the differential voltage appearing on the inductor. Here, for ten pulses, voltage swings within a bounded 3.4 V magnitude around 0 V – this is clearly set by the fixed 3.4 V output. On the eleventh pulse, the swing extends to a peak of around 4.4 V before falling rapidly to zero (with heavy ringing). This last pulse occurs when hitting the ISL9120's hysteretic voltage limit.

For each inductor voltage pulse, the inductor current follows a linear ramp. Each current pulse 'grows' the positive-going voltage ramp on the output capacitor (C2 in fig. 1a) as energy is transferred from inductor to capacitor (red trace).

PFM pulses stop when V_{OUT} reaches the upper hysteretic threshold of the regulator. Device data indicates that this is at a point 1.5 % above the nominal output. At a fixed 3.4 V output, that implies approximately 50 mV above it (i.e. at 3.45 V). As switching stops, V_{OUT} decays back to nominal, at which point PFM can start over.

The cyclical switching creates the characteristic sawtooth output ripple waveform riding on the fixed 3.4 V DC. The red trace shows that the ripple has a magnitude of about ± 20 mV – slightly better than the 50 mV predicted above. At this operating point, the switching interval is 6.36 μ s (157 kHz).

Finally, note the small perturbations on the positive-going edge of the ripple waveform. Rapidly chopped voltages across inductors cause electrical noise. It is clear that this is the origin of this output noise. There's obvious time correlation between the red and green traces. Viewing the blue (inductor current) trace adds further weight to this conclusion.

There's a fair bit of ringing evident on the inductor voltage waveform when the differential voltage hits zero volts. Clearly, the passive probe used to make this measurement is loading the tank formed between itself and the inductor. This is to be expected given the inductor is a tiny 1 μ H.

What happens at substantially lower loads?

Operating conditions remain constant in the following plot (fig. 6) except for a 20x reduction in load current to 25 mA:

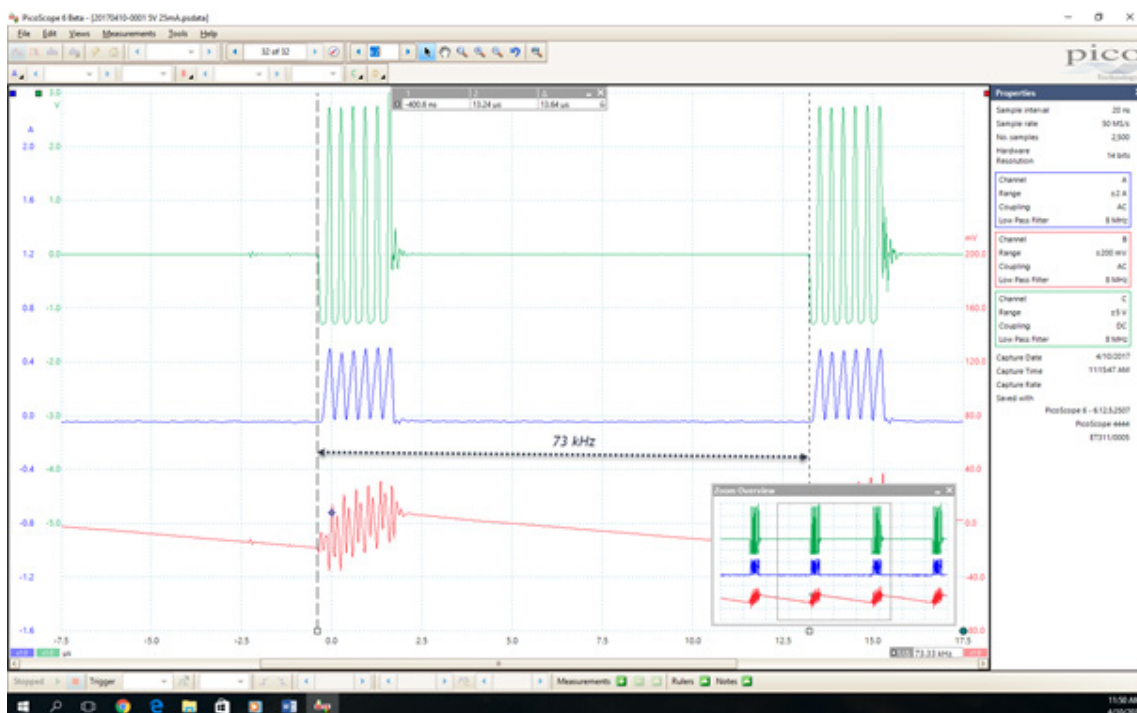


Figure 6 Step-down operation ($V_{in} = 5$ V, $V_{out} = 3.4$ V and $I_{out} = 25$ mA)

Unsurprisingly, we see comparable inductor behavior with similar signal amplitudes. That said, there is no dc offset component to the inductor current in light load conditions. However, as the load drops, the PFM burst interval has extended. This is caused by the significantly lower load energy demanded.

Only six PFM pulses occur now, but with a significantly extended off time between them. This difference is reflected in a slower output ripple rate - which has doubled to 13.7 μ s (73 kHz). Note that the ripple amplitude has halved to only ± 13 mV.

Interim conclusion – step-down mode

For PFM regulators, light loads result in a reduced output ripple frequency and voltage amplitude. Time between PFM pulse bursts increases with lighter loads. Off time extends to enhance low-load efficiency by limiting the dynamic switching losses that are typical of fixed frequency, PWM (pulse width modulation) regulators.

Now let's consider step-up operation.

Step-up operation ($V_{IN} < V_{OUT}$).

- Set-up: $V_{in} = 2.0\text{ V}$, $V_{out} = 3.4\text{ V}$ and $I_o = 250\text{ mA}$
- Traces:
 - o **Red:** output voltage ripple = 64 mV
 - o **Green:** inductor differential voltage (DC coupled)
 - o **Blue:** inductor current

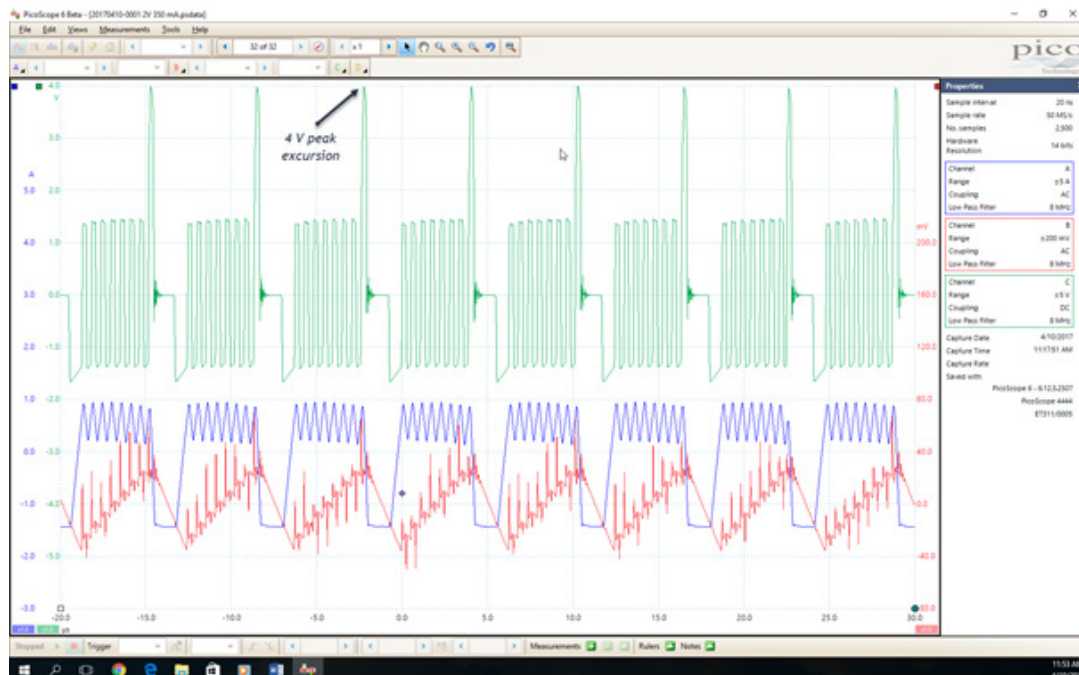


Figure 6 Step-down operation ($V_{in} = 5\text{ V}$, $V_{out} = 3.4\text{ V}$ and $I_{out} = 25\text{ mA}$)

This time around, the regulator works close to its minimum input voltage. Careful inspection of the waveform (fig. 7) shows that inductor voltage behavior remains similar to that of the step-down case.

Inductor current ramp up is clearly visible in blue. Inductor current swings $\pm 300\text{ mA}$ over seven pulses prior to hitting the eighth pulse, at which point the regulator's upper hysteresic limit is hit. The inductor current collapses, resulting in the negative going swing of the output ripple before the PFM process starts over.

Bypass operation ($V_{in} \approx V_{out}$)

- Static set-up conditions: $V_{in} = 3.45\text{ V}$, $V_{out} = 3.4\text{ V}$, with no load
- Traces:
 - o **Red:** output voltage ramp
 - o **Green:** input current peaks
 - o **Blue:** inductor current

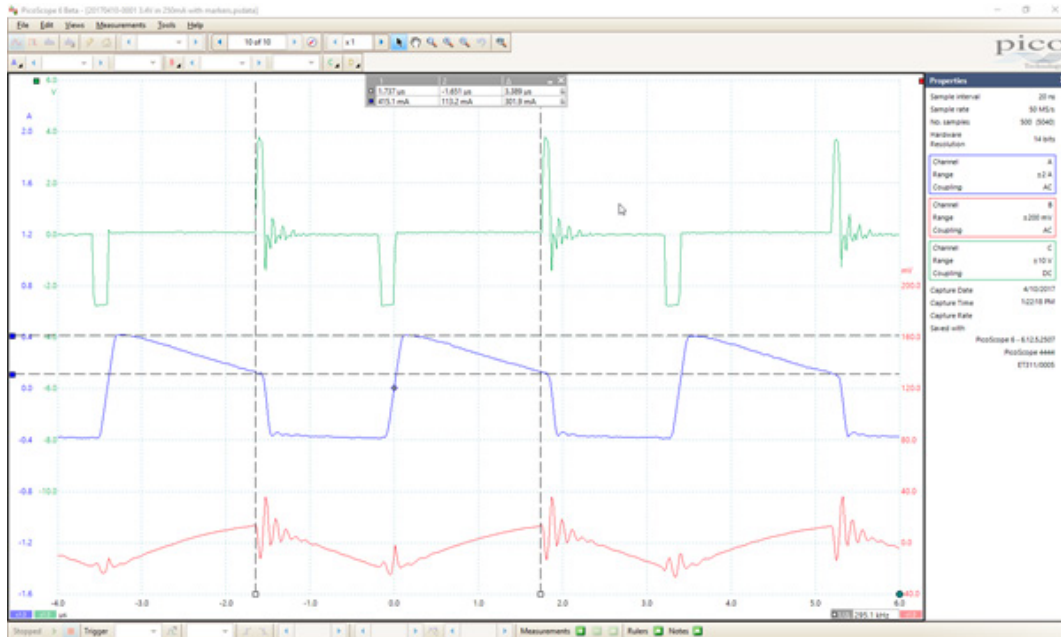


Figure 6 Bypass operation ($V_{in} = 3.4\text{ V}$, $V_{out} = 3.4\text{ V}$, 250 mA load)

This trace (fig. 8) shows operation when the input closely matches the output voltage – i.e. when working in bypass mode. The upper trace reveals short positive and negative going transient voltages swing across the inductor.

This time the inductor current looks markedly different.

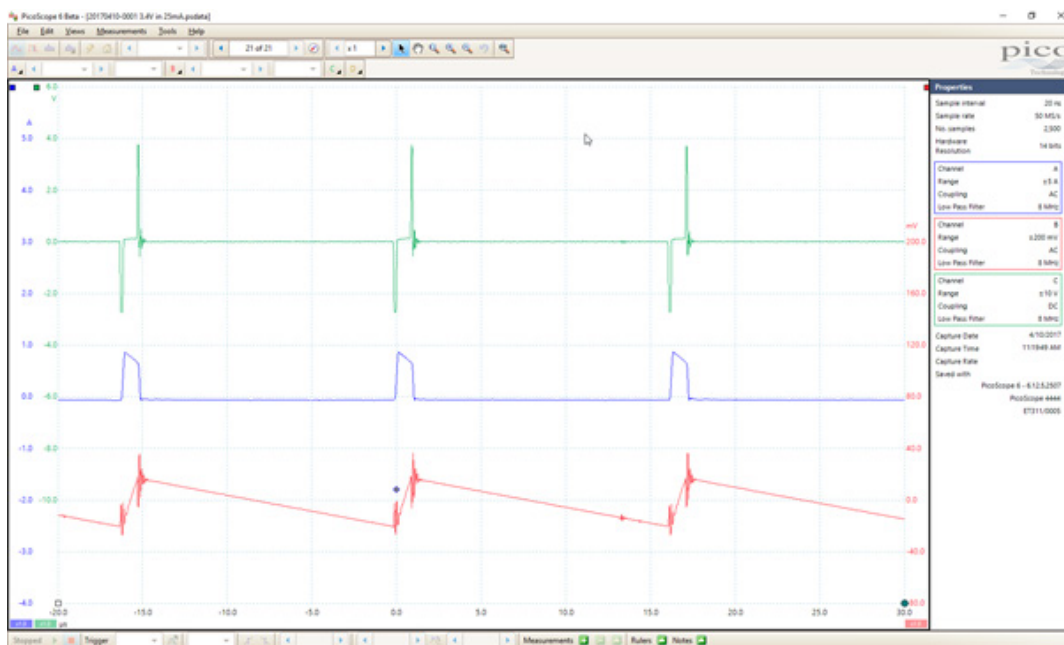


Figure 9 Bypass mode with 25 mA load

Rulers in fig. 8 reveal the negative going edge of the inductor current waveform is approximately 300 mA – in line with other modes. This edge represents energy tapped off from the inductor charging the output capacitor, causing the upswing in ripple voltage. The switch frequency is 295 kHz.

When the PFM switch is turned on, the inductor current rapidly falls by about -500 mA. In this case, ringing occurs on the falling edge of the output ripple waveform. In common with other operating modes, lowering the load causes the expected drop in switching frequency. With a 25 mA load shown (fig. 9) the frequency falls to 62 kHz.

Conclusion

Being able to view true differential signals, assisted by the high common mode rejection of the PicoScope 4444, aids rapid system debug of systems with floating nodes. In the case of a PFM regulator, inductor current flow and its impact on output voltage ripple performance were established. This demonstrated the effect of the device's control system: namely a fall in number of PFM pulses and switching rate leading a simultaneous drop in ripple frequency and amplitude at lighter loads, irrespective of operating mode.

Probing the inductor helped identify the source of output voltage noise, namely that of the PFM current pulses acting on itself. It became clear that passively probing the small inductor used by the regulator loaded the circuit, aggravating the ringing seen in several traces.

Not immediately apparent from reading this is the fact that the PicoScope 4444 provides several features that simplified the performance of tests described in this article. It is an important point to be touched on in a future feature.

Finally, though the type of switcher used for this review is highly efficient and easy to deploy, it does not suit all applications. Variable frequency operation makes EMI control a challenge. For this reason, PFM regulators are less widely used in precision and sensitive radio applications.

For more information on the PicoScope 4444 please visit our website at www.picotech.com



References

- For more insights into the operation of the ISL9120 please refer to the device datasheet

Many sources of information on hysteretic switchers can be found online including the following:

- "Circuit Tradeoffs Minimize Noise in Battery-Input Power Supplies." Maxim Integrated. Maxim Integrated, 22 Jan. 2001. Web. 10 Mar. 2017.
<<https://www.maximintegrated.com/en/app-notes/index.mvp/id/653>>.
- "Characteristics and Evaluation Method of Switching Regulators." Tech Web. Rohm Co. Ltd, 14 Mar. 2016. Web. 10 Mar. 2017.
<http://micro.rohm.com/en/techweb/knowledge/dcdc/dcdc_sr/dcdc_sr01/897>

Pico Technology
James House
Colmworth Business Park
ST. NEOTS
PE19 8YP
United Kingdom

☎ +44 (0) 1480 396395
☎ +44 (0) 1480 396296
✉ sales@picotech.com

Pico Technology
320 N Glenwood Blvd
Tyler
Texas 75702
United States

☎ +1 800 591 2796
☎ +1 620 272 0981
✉ sales@picotech.com

Pico Technology GmbH
Im Rehwinkel 6
30827 Garbsen
Germany

☎ +1 800 591 2796
☎ +1 620 272 0981
✉ info.de@picotech.com

